The Coupling of Surface and Internal Gravity Waves: Revisited

KENNETH M. WATSON

Marine Physical Laboratory, Scripps Institution of Oceanography, University of California, San Diego, California

(Manuscript received 29 September 1988, in final form 13 September 1989)

ABSTRACT

A new investigation is made of internal wave generation by surface waves. Previous theories are put into a unified form that includes a model of surface wave damping. Calculations using the complete theory, which do not seem to have been made previously, indicate that for wind speeds between 7 and 20 m s^{-1} the internal wave field *loses* about 10^{-4} W m^{-2} to the surface wave field. This would lead to a decay time of about 10 days for the high frequency portion of the internal wave field if an energy source were not available to maintain it. Possible sources for this energy are discussed. In contrast to this result for wind waves, a strong, highly collimated ocean swell can lead to rapid growth of high frequency internal waves. The effects of nonlinear surface wave modulation and wave blocking are also discussed.

1. Introduction

According to the model of Garrett and Munk (1972a), the nominal energy in the internal wave field is about 3 kJ m^{-2}. Except for local variations this appears to be more-or-less steady, which has led to the view that generation and dissipation mechanisms balance each other. Garrett and Munk (1972b) estimated from turbulent fluxes that the dissipation rate for the internal wave (IW) field is in the range of 10^{-3} W m^{-2}. Dissipation rates for small scale turbulence (assumed to be fed by internal waves) observed, for example, by Garget et al. (1981) and by Osborn (1978) imply dissipation rates in the range of 10^{-3} to 10^{-4} W m^{-2}. Vertical fluxes of IW energy observed by Leaman and Sanford (1975) and by Leaman (1976) are also in this range. These rates suggest that the IW field would decay in 10 to 100 days if it were not maintained by external sources. Further observations by Lueck et al. (1983), by Gregg et al. (1986), and by Gregg (1987, 1989) lead to estimates of about 50 to 100 days for the IW decay time.

Theoretical calculations of turbulent fluxes within the IW field by McComas (1978), McComas and Muller (1981), and Pomphrey et al. (1980) predict dissipation rates in the range of 10^{-3} to 10^{-4} W m^{-2}. Careful predictions by Flattè et al. (1985) give values toward the lower end of this range, in agreement with Gregg (1989).

A number of plausible mechanisms have been proposed for the generation of internal waves. Bell (1975) has suggested that large scale flow over topography can be a significant source of IW energy. Bell (1978) has also concluded that inertial oscillations of the upper ocean can generate internal waves. Kanthu (1979) has investigated mixed layer turbulence as a generation mechanism. Mesoscale flow as a source of IW energy has been studied by Watson (1985). Each of these mechanisms appears able to account for much of the energy in the IW field.

Striking visual evidence of the interaction of internal waves with surface waves has been often noted (for example, see Hughes and Grant 1978; Phillips 1973; Hughes 1978; Apel et al. 1975; Curtin and Mooers 1975; Fu and Holt 1984). This interaction has led to a number of calculations of the rate of generation of the IW field by surface waves.

Theoretical models for a "wave triad" consisting of two surface waves and one internal wave have been developed by Ball (1964), Thorpe (1966), and Brekhovskikh et al. (1972). Energy transfer occurs when a frequency resonance condition is met.

Calculations of the transfer of energy from a surface wave (SW) spectrum to internal waves have been given by Kenyon (1968), Watson et al. (1976), Olbers and Herterich (1979), and Dysthe and Das (1981). Kenyon used a constant N (i.e., Väisälä frequency) profile. Olbers and Herterich chose N to be constant in a prescribed depth interval and to vanish outside this interval. Dysthe and Das (1981, hereafter DD) assumed N to vanish outside a thin thermocline region. Watson et al. (1976, hereafter WWC) chose N to vanish in a mixed layer, below which they used the Garrett–Munk (1972a) exponential scaling.

Olbers and Herterich (1979) made use of the spectral transfer equations of Hasselmann (1967). They con-

Corresponding author address: Dr. Kenneth M. Watson, University of California, San Diego, Marine Physical Laboratory, Scripps Institution of Oceanography, San Diego, CA 92152-6400.

sidered a mechanism of "spontaneous creation" by which pairs of surface waves generate internal waves. This mechanism does not require that internal waves be initially present. Dysthe and Das describe another mechanism by which a weak IW grows (or decays) exponentially through interaction with a pair of surface waves. They refer to this as "modulation interaction" or "modulational instability."

Olbers and Herterich (1979) concluded that the transfer rates for the *spontaneous creation* mechanism are relatively insensitive to the detailed form of the SW spectrum, but are sensitive to the wind speed. A large Väisälä frequency, a thin mixed layer, or strong winds were required to give significant IW growth rate, however.

Dysthe and Das performed calculations for only a narrow band SW system. They concluded that the energy rate for *modulation interaction* mechanism is very sensitive to the form of the SW spectrum and that a very narrow angular spread is required to give significant growth rates of the IW amplitudes.

The mode coupling equations of WWC were expressed in the form of Hamilton's equations. They obtained an analytic expression for the IW growth rate using a "locked phase assumption." This gave a significant energy transfer rate, but because of the locked phase approximation could be considered as only an upper limit on the IW growth rate. Watson et al. also performed a numerical integration of their equations. This was criticized by Olbers and Herterich (1979) as ignoring the detuning effects of SW dissipation processes. Because of computational limitations, WWC chose a narrow band SW spectrum similar to that shown by DD to give high energy transfer rates.

The conclusions from these calculations has been that SW–IW interactions cannot account for the energy needed to maintain the IW field. It appears however that, although the theory has been well developed, detailed calculations of the SW–IW energy exchange have not been made. Studies have not been made that include simultaneously both the spontaneous and modulation mechanisms, nor have comparisons of the relative importance of these been given.

The purpose of this paper is to provide such calculations that include both the modulation and the spontaneous mechanisms and to do these for environmental conditions of physical interest. In contrast to what has sometimes been expected, we find rather rapid energy transfer rates, but predominantly a transfer of energy from the IW field to the SW field.[1] This transfer of energy is significant, however, only for the long vertical wavelength IW modes having frequencies greater than about a tenth of the upper ocean Väisälä frequency. In this band and for wind speeds in the 7 to 20 m s^{-1} range the predicted time for IW decay is a few days. Expressed differently, for a Garrett–Munk spectrum the power delivered to the SW field at the expense of the IW field is about 10^{-4} W m^{-2}. This is not of course a significant energy source for the wind waves, but (as we shall discuss later) it does raise a question as to the source for the IW energy in this band.

For a wind increasing above 15 m s^{-1} there is a tendency in some spectral domains for transfer of energy to the IW field, although at even 20 m s^{-1} the net transfer is to the SW field.

The theories of WWC, DD, and Olbers and Herterich (1979) are described (without derivation)[2] in sections 2 and 3. An innovation in the present work is to take account of surface wave dissipation. This dissipation broadens the triad resonance condition of the previous theories. This broadening has some numerical impact, but does not significantly change our conclusions. The calculations described in the paragraph above are presented in Section 4. In Section 5 we show the implications of some calculations of IW generation by ocean swell, which can effectively stimulate IW growth. Finally, in Section 6 some implications of nonlinear SW modulation are described.

2. Notation and ocean model

In this section we shall review for later use certain properties of linear surface and internal waves (for a more detailed description of the linear wave fields see, for example, Phillips 1977). Where appropriate, we will follow the notation of WWC.

Capillary waves will be excluded from our model. Characteristic IW frequencies Ω are assumed to be small compared to frequencies ω of the interacting SW field, but much larger than the inertial frequency. Similarly, horizontal IW wavenumbers K are assumed to be small compared to wavenumbers k of the SW field:

$$\Omega \ll \omega$$
$$K \ll k. \tag{2.1}$$

The undisturbed surface of the ocean is assumed to coincide locally with the plane $z = 0$ of a rectangular coordinate system. The ocean bottom is assumed to coincide with the plane $z = -B_b$. The Väisälä frequency $N(z)$ is assumed to vanish in a mixed layer of domain $-D < z < 0$. It will be supposed that D is large enough that surface wave currents can be neglected for $z < -D$. Specific models for $N(z)$ in the domain $-D > z > -B_b$ will be introduced when calculations are presented.

Following the notation of WWC, for *linear* internal

[1] We emphasize that our present calculations do not disagree with other calculations of which we are aware. The pertinent calculations seem not to have been done before.

[2] A very simple derivation of the energy transfer resulting from the modulation mechanism is given Section 3, using arguments of energy conservation.

waves we expand the vertical component of velocity in the form

$$w_i(\mathbf{x}, z, t) = \sum_{j=i}^{\infty} \sum_{\mathbf{K}} e^{i\mathbf{K}\cdot\mathbf{x}} A_{j,\mathbf{K}}(t) W_{j,K}(z). \quad (2.2)$$

The sum on K represents a Fourier expansion in some conveniently chosen rectangular Area A_0. The symbol j labels vertical mode numbers. The vertical mode function $W_{j,K}(z)$ is obtained from the equations

$$W_{j,K}(z) = K \sinh(Kz), \quad -D < z \leqslant 0,$$
$$W''_{j,K}(z) + K^2(N^2/\Omega^2 - 1)W_{j,K} = 0, \quad -B_b < z < -D \quad (2.3)$$

where $W'' = d^2W/dz^2$ and Ω is the angular frequency of the mode (j, K). At the ocean bottom we have the boundary condition

$$W_{j,K}(-B_b) = 0.$$

The rigid-lid approximation has been used to give the boundary condition at $z = 0$ in (2.3). Olbers and Herterich (1979) have discussed the validity of this and the Bousinesq approximation for the present application. We have used their analysis to explicitly verify the validity of these approximations for the parameter ranges used in our calculations. For linear waves we have the relation

$$\ddot{A}_{j,\mathbf{K}} = -\Omega^2(j, K)A_{j,\mathbf{K}} \quad (2.4)$$

where $\ddot{A} \equiv d^2A/dt^2$.

We shall encounter the integrals

$$\int_{-B_b}^{0} N^2 W_{j',K} W_{j,K} dz = \delta_{j,j'} V_{j,K} N_0^2/B. \quad (2.5)$$

Here N_0 and B are convenient scale parameters for N and for the vertical scale of stratification, respectively. The quantity $V_{j,K}$ above is dimensionless. It will be seen to represent a kind of IW inertial response to SW driving.

The horizontal component of the IW current is

$$\mathbf{u}(\mathbf{x}, z, t) = \sum_{j,\mathbf{K}} i\mathbf{K} A_{j\mathbf{K}} W'_{j,K} e^{i\mathbf{K}\cdot\mathbf{x}}/K^2. \quad (2.6)$$

It is convenient to write

$$iK^{-1}A_{j,\mathbf{K}} = \tfrac{1}{2}[\hat{U}(j, \mathbf{K}) \exp(-i\Omega(j, K)t) - \hat{U}^*(j, -\mathbf{K}) \exp(i\Omega(j, K)t)]. \quad (2.7)$$

Then at the surface $z = 0$ we may use (2.4) to express (2.6) in the form

$$\mathbf{U}(\mathbf{x}, t) = \sum_{j,\mathbf{K}} \hat{\mathbf{K}}[\hat{U}(j, \mathbf{K}) \exp(i(\mathbf{K}\cdot\mathbf{x} - \Omega t)) + \text{c.c.}]/2. \quad (2.8)$$

The internal wave energy/unit area in the mode (j, K) is

$$\hat{E}_i(j, \mathbf{K}) = \frac{\rho_0 N_0^2 V_{j,K}}{2B\Omega^2 K^2} \left|\hat{U}(j, \mathbf{K})\right|^2, \quad (2.9)$$

where ρ_0 is the density of sea water (say, in the mixed layer). The spectrum of internal wave energy $E_i(j, \mathbf{K})$ is obtained from (2.9) as

$$\int E_i(j, \mathbf{K}) d^2K = \sum_{\mathbf{K}} \hat{E}_i(j, \mathbf{K}). \quad (2.10)$$

The corresponding action/unit area is

$$F_i(j, \mathbf{K}) = E_i(j, \mathbf{K})/\Omega(j, K). \quad (2.11)$$

For the calculations to be given later we shall need a model for E_i, for which we take, unless specified otherwise, the venerable Garrett–Munk spectrum of Munk (1981). Since we are interested only in IW frequencies much larger than the inertial frequency, we write this as

$$E_i(j, K) = \frac{0.013\rho_0 N_0^2 \xi_0^2 j}{2\pi K^3(1 + j^2/9)} \quad (2.12)$$

valid for $KB \gg f_0\pi j/N_0$, where f_0 is the inertial frequency. We recognize that (2.13) does not always describe very well internal wave observations in the upper ocean (see Pinkel 1985). We do not think, however, that our conclusions are sensitive to details of the IW spectrum.

For linear surface waves we write the vertical displacement and velocity potential at $z = 0$ in the form

$$\zeta_s(\mathbf{x}, t) = -\sum_{\mathbf{k}} [B_{\mathbf{k}} e^{i\mathbf{k}\cdot\mathbf{x}} - \text{c.c.}]/(2i\sqrt{\rho_0 V_k}),$$
$$\phi_s(\mathbf{x}, t) = \sum_{\mathbf{k}} \sqrt{V_k/(2\rho_0)}\,[B_{\mathbf{k}} e^{i\mathbf{k}\cdot\mathbf{x}} + \text{c.c.}]. \quad (2.13)$$

Here $V_k = \sqrt{g/k}$ is the surface gravity wave phase speed. The surface wave spectrum of action/unit area is F_s. This may be obtained from (2.13) using the Wigner (1932) relation

$$\int d^2k F_s(\mathbf{x}, \mathbf{k}, t) = \sum_{\mathbf{k}} \sum_{\mathbf{l}} e^{i\mathbf{l}\cdot\mathbf{x}} \langle B_{\mathbf{k}+1/2} B^*_{\mathbf{k}-1/2} \rangle \quad (2.14)$$

where $\langle\ \rangle$ represents an ensemble average over many realizations of the SW field. The corresponding SW energy spectrum is

$$E_s(\mathbf{x}, \mathbf{k}, t) = \omega_k F_s(\mathbf{x}, \mathbf{k}, t) \quad (2.15)$$

where $\omega_k = \sqrt{gk}$ is the angular frequency corresponding to wavenumber k.

It is convenient to introduce an ambient SW field for which we can use one of the current equilibrium models. We shall denote the action density spectrum for this ambient field by $F_a(\mathbf{k})$. The ambient spectrum

of vertical displacement Ψ_a is expressed in terms of the action density with the relation

$$F_a(\mathbf{k}) = \rho_0 V_k \Psi_a(\mathbf{k}). \tag{2.16}$$

The ratio of the actual to the "ambient" spectrum represents the SW modulation M:

$$F_s(\mathbf{x}, \mathbf{k}, t) = M(\mathbf{x}, \mathbf{k}, t) F_a(\mathbf{k}). \tag{2.17}$$

We shall see in the next section that for the modulation mechanism it is M that can be considered as the *driver* of the IW field.

For the calculations presented in this paper we shall use the wind wave spectral model of Donelan et al. (1985) and Phillips (1985):

$$\Psi_a(\mathbf{k}) = S(k) G(\theta - \theta_w). \tag{2.18}$$

Here θ is the angle of the vector $\mathbf{k}$ with respect to the direction of $\mathbf{K}$ and θ_w is the corresponding direction of the wind vector. The function S is

$$S(k) = \frac{A}{k^{3.5}\sqrt{k_*}} e^{-\Gamma},$$

$$\Gamma = 0.6(k_*/k)^2 - 0.5 \exp[-1.2(1.2\sqrt{k/k_*} - 1)^2],$$

$$k_* = g/W^2, \quad A = 3 \times 10^{-3}, \tag{2.19}$$

and W is the wind speed. The "spreading function" of Donelan et al. (1985) is

$$G(\theta - \theta_w) = \sigma \operatorname{sech}^2[\sigma(\theta - \theta_w)]/2. \tag{2.20}$$

The Donelan model used for the parameter σ is

$$\sigma = \begin{cases} 2.9(k_*/k)^{0.67}, & \text{for } k/k_* < 4 \\ 1.2, & \text{for } k/k_* > 4. \end{cases} \tag{2.21}$$

We shall also consider a "collimated" model for which

$$\sigma = 8. \tag{2.22}$$

Our calculated results will be seen to be rather sensitive to the spreading function used, but do not seem very sensitive to modest changes in S. Omitting the "JONSWAP peak enhancement" in (2.19) or using a k^{-4} spectrum in the equilibrium range does not modify our results significantly.

3. The interaction between surface and internal waves

In this section we shall present the equations that describe the response of the IW field to SW forcing. The derivations given by DD and WWC lead to equivalent results for the modulation mechanism, which we now quote without derivation. (Since the form in which we express the modulation mechanism is somewhat different from that given by WWC and DD, we show in the Appendix how to obtain this specific form using expressions derived in WWC.) A very simple derivation is given at the end of this section, however, for the transfer of energy between the IW and SW fields, as implied by the modulation mechanism.

The equations of Olbers and Herterich (1979) describing the spontaneous model are also quoted in this section, re-expressed in the present notation.

The SW and IW fields are treated as linear, except for the coupling between them. This coupling is assumed to be weak in the sense that the linear wave frequency Ω is large compared to the evolution rate of the amplitudes $\hat{U}(j, \mathbf{K})$:

$$\Omega \gg |\dot{\hat{U}}/\hat{U}|. \tag{3.1}$$

The nonlinear coupling is evaluated in lowest order as a triad wave interaction. A typical triad from a field of interacting waves would include two surface waves of wavenumbers $\mathbf{k}$ and $\mathbf{k}'$ and an internal wave of mode $(j, \mathbf{K})$. Energy exchange among these waves occurs when a resonance condition is met:

$$\mathbf{k} - \mathbf{k}' = \mathbf{K},$$

$$\omega_k - \omega_{k'} = \Omega(j, K). \tag{3.2}$$

Higher order resonances, involving harmonics of the linear wave frequencies, can also transfer energy. When condition (3.1) is satisfied, we do not expect significant transfer rates from these higher order interactions. We shall see that SW relaxation mechanisms can lead to more general conditions than (3.2) for energy exchange, however.

Because of the conditions (2.1) we may rewrite the second equation above as

$$\mathbf{c}_g(\mathbf{k}) \cdot \hat{\mathbf{K}} = c_I, \tag{3.3}$$

where $c_i = \Omega/K$ is the IW phase velocity and c_g is the SW group velocity. This is the condition that the component of SW group velocity parallel to K match the IW phase velocity. An obvious generalization of (3.3) is the expression

$$[\mathbf{c}_g(\mathbf{k}) + \mathbf{U}] \cdot \hat{\mathbf{K}} = c_I. \tag{3.4}$$

As will be discussed in more detail in Section 6, (3.4) is the condition that an overtaking SW will be turned back, or *blocked,* by the IW generated surface current U. In the case of sufficiently weak interactions (3.3) and (3.4) are equivalent (recall that $|U|$ must be significantly less than c_I if the IW field can be treated as linear). The relation (3.4) leads us to anticipate that SW blocking plays a role in the energy transfer between the two wavefields.

The derivations of the modulation mechanism given by WWC and DD lead to an expression for the rate of change of the IW current amplitude introduced in (2.9):

$$\dot{\hat{U}}(j, \mathbf{K}) = -i\left(\frac{\Omega^3 KB}{N_0^2 \rho_0 V_{j,K}}\right)\mathbf{K}\cdot\int d^2k\mathbf{k}\int\frac{d^2x}{A_0}$$
$$\times \exp[-i(\mathbf{K}\cdot\mathbf{x} - \Omega t)]F_s(\mathbf{x}, \mathbf{k}, t). \quad (3.5)$$

Here A_0 is the rectangular area within which the Fourier expansion (2.4) was introduced. [As noted earlier, we show in the Appendix how Eq. (2.29) of WWC may be transformed into the form used here.] We may rewrite (3.5) using the modulation function M of (2.17),

$$\dot{\hat{U}}(j, \mathbf{K}) = i\left(\frac{\Omega^3 KB}{N_0^2 \rho_0 V_{j,K}}\right)\mathbf{K}\cdot\int d^2k\mathbf{k}\int d^2x\Big/A_0$$
$$\times \exp[-i(\mathbf{K}\cdot\mathbf{x} - \Omega t)][M(\mathbf{x}, \mathbf{k}, t) - 1]F_a(\mathbf{k}). \quad (3.6)$$

This shows explicitly how modulation of the SW spectrum is required to excite the IW field.

The rate of change of the IW energy is obtained from (2.9) and (3.5) as

$$\dot{E}_i(j, \mathbf{k}) = i\left(\frac{\hat{\mathbf{K}}}{2}\right)\cdot\int d^2k\mathbf{k}\int\frac{d^2x}{A_0}F_s(\mathbf{x}, \mathbf{k}, t)$$
$$\times \Omega[\hat{U}\exp[i(\mathbf{K}\cdot\mathbf{x} - \Omega t)] - \text{c.c.}]. \quad (3.7)$$

Using the condition (3.1) and (2.10) we can put this in the compact form

$$\dot{E}_i = \sum_{j,\mathbf{K}}\dot{E}_i(j, \mathbf{K})$$
$$\approx -\int d^2k\mathbf{k}\cdot\int\frac{d^2x}{A_0}\dot{\mathbf{U}}(\mathbf{x}, t)F_s(\mathbf{x}, \mathbf{k}, t). \quad (3.8)$$

To continue, we need a model or a prescription for calculating F_s. There are several possibilities: 1) The IW field surface current can modulate the SW field. An equation from which to determine F_s from $\hat{U}$ will close the system, permitting $\hat{U}$ and F_s to be calculated simultaneously. This is the approach used by DD and by WWC (with their analytic calculation). 2) The SW modulation may be determined by external environmental factors. This might be due to wind variability (for example, see Gill 1984), spatial variation of swell, Langmuir circulation, etc. An example, assuming a modulated ocean swell, will be described in section 5. 3) Modulation can also result from random statistical fluctuations of the SW field.

To describe the first of these modulation possibilities we shall adopt a simple, often used model that takes account of the inequalities (2.1). In the ray path approximation we can write (for example, see Hasselmann 1968)

$$\left[\frac{\partial}{\partial t} + \dot{\mathbf{x}}\nabla_{\mathbf{x}} + \dot{\mathbf{k}}\cdot\nabla_{\mathbf{k}}\right]F_s(\mathbf{x}, \mathbf{k}, t) = S(\mathbf{x}, \mathbf{k}, t). \quad (3.9)$$

Here

$$\dot{\mathbf{x}} = \nabla_{\mathbf{k}}H, \quad \dot{\mathbf{k}} = -\nabla_x H,$$
$$H = \omega_k + \mathbf{k}\cdot\mathbf{U}. \quad (3.10)$$

The source term S is often expressed as

$$S = S_{nl} + S_w + S_d, \quad (3.11)$$

where S_{nl} represents nonlinear SW–SW interactions (Hasselmann 1967 or 1968), S_w represents wave excitation by the wind, and S_d represents wave damping due to viscosity.

Equations (3.9) and (3.11) are overly complex for our current study [see, however, van Gastel (1987), who investigated SW modulation using this full set of equations for capillary waves], so we shall adopt a model for S introduced by Hughes (1978) and by Phillips (1984). We set

$$S = -\beta(k)(F_s - F_a), \quad (3.12)$$

which is the form of the Hughes and Phillips models when $|F_s - F_a| \ll F_a$. The non-negative constant β used in this paper is that deduced by Watson (1986). His calculations may be scaled in the approximate form

$$\beta(k) = \omega_k\exp(-G(p)),$$
$$p = W/V_k,$$
$$G = \frac{14.5C(p)}{0.4 + p^{0.579}},$$
$$C(p) = \begin{cases} 1, & \text{if } p < 15, \\ \dfrac{5}{p - 10}, & \text{if } p > 15. \end{cases} \quad (3.13)$$

When the action source term S in (3.9) is negligible, we expect the total energy of both wave fields to be constant. (The Hamiltonian formulation of WWC assures energy conservation when there is no SW damping.) To verify this, we write

$$\int\frac{d^2x}{A_0}\int d^2k\omega_k\left[\frac{\partial}{\partial t} + \dot{\mathbf{x}}\cdot\nabla_{\mathbf{x}} + \dot{\mathbf{k}}\cdot\nabla + \dot{k}\cdot\nabla_{\mathbf{k}}\right]F_s = 0,$$

or

$$\dot{E}_s + \int\frac{d^2x}{A_0}\int d^2k[(\dot{x}\cdot\nabla_x + \dot{k}\cdot\nabla_k)(\omega_k \times F_s)$$
$$- F_s(\nabla_{\mathbf{k}}\omega_k)\cdot\dot{\mathbf{k}}] = 0.$$

Then

$$\dot{E}_s = \int\frac{d^2x}{A_0}\int d^2k\dot{\mathbf{k}}\cdot\mathbf{c}_g(\mathbf{k})F_s. \quad (3.14)$$

Now

$$\dot{\mathbf{k}}\cdot\mathbf{c}_g = -\mathbf{c}_g\cdot\nabla_x(\mathbf{U}\cdot\mathbf{k}) \approx \mathbf{k}\cdot\dot{\mathbf{U}},$$

where we have made use of the condition (3.3). Thus (3.14) becomes

$$\dot{E}_s = \int d^2x/A_0 \int d^2k\mathbf{k}\cdot\dot{\mathbf{U}}F_s(\mathbf{x}, \mathbf{k}, t) = -\dot{E}_l. \tag{3.15}$$

The last form follows from energy conservation. In obtaining (3.15) we have made use of the condition (3.3).

We see that this provides an alternate derivation of (3.8). When SW damping is significant, (3.15) remains valid for the IW energy rate, but an additional term is added to the SW energy rate of change.

Equations (3.5) and (3.14) describe the response of the IW field to a modulated SW field. When this modulation is driven by the IW field, (3.9) may be used (this is the case explicitly considered by WWC and DD, who did not include SW relaxation, however) to close the set of equations.

Olbers and Herterich (1979) presented calculations using the "spontaneous creation" mechanism. (We use this term since internal wave energy does not have to be present for this process to work.) The rate at which the IW field receives energy from the SW field, as obtained by Olbers and Herterich (1979), is

$$\left.\frac{\partial E_l(j, K)}{\partial t}\right)_s = \frac{4\pi\alpha g\rho_0 N_0\Omega}{KB^2}\int d^2k(k_x^2/k)\Psi_a(\mathbf{k}) \times \Psi_a(\mathbf{k}')\delta(\omega_k - \omega_{k'} - \Omega). \tag{3.16}$$

Here the x-axis has been chosen as the direction of the vector $\mathbf{K}$ and $\mathbf{k}' = \mathbf{k} - \mathbf{K}$, $\Omega = \Omega(j, K)$. The dimensionless quantity α is

$$\alpha = \frac{(\Omega KB/N_0)^3}{2V_{j,K}}, \tag{3.17}$$

where $V_{j,K}$ is given by (2.7).

In the next section we shall present calculations of the energy exchange between SW and IW fields using (3.5) and (3.9) for the modulation mechanism and (3.16) for the spontaneous mechanism. In Section 5 we discuss IW generation by a naturally modulated ocean swell. Finally, in section 6 we investigate the case that the SW field is strongly modulated by a packet of internal waves.

4. The case of weak modulation

When the IW surface current is sufficiently weak we may linearize (3.9) in U. In this case there is no coupling among the modes and it suffices to consider only a single IW mode, say (j, K). We may take K parallel to the x-axis and write

$$\mathbf{U}(\xi, t) = \mathbf{i}[\hat{U}(t)e^{iK\xi} + \text{c.c.}]/2, \tag{4.1}$$

where $\mathbf{i}$ is a unit vector parallel to the x-axis and $\xi = x - c_l t$. We shall also omit writing the (j, K) label on U, etc., except where it is needed for clarity.

The distortion in F_a due to the IW current is

$$F'(\xi, \mathbf{k}, t) \equiv F_s - F_a, \tag{4.2}$$

and the linearized form of (3.9) is

$$\left[\frac{\partial}{\partial t} + (c_x - c_l)\frac{\partial}{\partial\xi}\right]F' = k_x\frac{\partial U}{\partial\xi}\frac{\partial F_a}{\partial k_x} - \beta F' \tag{4.3}$$

where c_x is the x-component of c_g. It is convenient to introduce positive and negative frequency parts of F' in (4.3)

$$F' = [H(\mathbf{k}, t)e^{iK\xi} + \text{c.c.}]/2,$$

so (4.3) becomes

$$\left[\frac{\partial}{\partial t} + \beta + iK(c_x - c_l)\right]H = iKk_x\frac{\partial F_a}{\partial k_x}\hat{U}. \tag{4.4}$$

Equation (3.9) for $\hat{U}$ can now be expressed as

$$\frac{\partial\hat{U}}{\partial t} = -[i\alpha N_0/(KB^2\rho_0)]\int d^2kk_xH, \tag{4.5}$$

where the dimensionless quantity α is given by (3.17).

We may suppose that $\hat{U}$ and H evolve from initial values $\hat{U}(0)$ and $H(k, 0)$ at time $t = 0$. An explicit solution to (4.4) and (4.6) is then readily obtained using a Laplace transform.

$$\bar{U} = \int_0^\infty e^{-pt}\hat{U}dt,$$

$$\bar{H} = \int_0^\infty e^{-pt}Hdt.$$

For the quantity $\bar{U}$ we find

$$[p - \alpha J]\bar{U} = \hat{U}(0) - i[\alpha N_0/(KB^2\rho_0)] \times \int d^2kk_xH(\mathbf{k}, 0)\Big/[p + \beta + iK(c_x - c_l)], \tag{4.7}$$

with

$$J = (N_0/B^2)\int\frac{d^2kk_x^2\dfrac{\partial}{\partial k_x}[V_k\Psi_a(\mathbf{k})]}{p + \beta + iK(c_x - c_l)}. \tag{4.8}$$

Here Ψ_a is the SW displacement spectrum (2.18).

The free response of the system is obtained from the equation

$$p = \alpha J. \tag{4.9}$$

It will be seen that $|p|$ is sufficiently small that the term p can be dropped in the denominator of (4.8). Also we need calculate only the real part of (4.9), which is then

$$\text{Re}(p) = (\alpha N_0\pi/B^2)\int d^2kk_x^2\left\{\frac{\partial}{\partial k_x}[V_k\Psi_a(\mathbf{k})]\right\} \times \Delta[K(c_x - c_l)] \tag{4.10}$$

where

$$\Delta = \frac{\beta/\pi}{\beta^2 + K^2(c_x - c_I)^2}. \quad (4.11)$$

When β is much less than Ω,

$$\Delta[K(c_x - c_I)] = \delta[K(c_x - c_I)]. \quad (4.12)$$

To be compatible with (3.16) we shall replace (4.10) by

$$\nu_m = 2\,\mathrm{Re}(p) \quad (4.13)$$

describing the rate at which IW energy grows. Olbers and Herterich (1979) also obtained, but did not discuss, a result equivalent to (4.10) and (4.12).

The mean IW growth rate, averaged over all K-directions (equivalent to averaging over all directions θ_w), is

$$\bar{\nu}_m = \frac{1}{2\pi}\int_{-\pi}^{\pi} \nu_m d\theta_w. \quad (4.14)$$

The rate at which energy is received in unit area of ocean, in mode j, and within the interval dK is

$$P_m(j, K)dK = 2\pi\bar{\nu}_m E_i(j, K)KdK. \quad (4.15)$$

For E_i we use (2.12).

To obtain a growth rate for the spontaneous mechanism we use (3.16):

$$\nu_s = \frac{\partial E_i(j, K)}{\partial t}\Big/ E_i(j, K)$$

$$= \frac{4\pi\alpha g\rho_0 N_0 \Omega}{KB^2 E_i}\int d^2k(k_x^2/k)\Psi_a(\mathbf{k})\Psi_a(\mathbf{k}') \times \Delta(K(c_x - c_I)). \quad (4.16)$$

Here for consistency we have replaced the δ-function in (3.16) by the function (4.11), for which plausible arguments may be given. The mean rate for all K-directions is

$$\bar{\nu}_s = \frac{1}{2\pi}\int_{-\pi}^{\pi} \nu_s d\theta_w. \quad (4.17)$$

The rate at which power is received per unit area by the IW field is then

$$P_s(j, K)dK = 2\pi\bar{\nu}_s E_i(j, K)KdK.$$

Net e-folding rates for the IW field are

$$\nu = \nu_m + \nu_s, \quad (4.18)$$

$$\bar{\nu} = \bar{\nu}_m + \bar{\nu}_s. \quad (4.19)$$

The total power received by the IW field per unit area is[3]

$$P(j, K) = P_m(j, K) + P_s(j, K). \quad (4.20)$$

Olbers and Herterich (1979) presented calculations for the spontaneous model using (3.16). They used a "box" Väisälä profile. (We have repeated selected examples of their calculations to compare numerical results, but have not systematically pursued this somewhat unphysical Väisälä profile.) An expression equivalent to (4.10) and (4.12) was used by DD to discuss IW generation by the modulation mechanism for a thin thermocline and a narrow band ocean swell.

A systematic investigation of the implications of (4.10) and (4.16) does not seem to have been made, perhaps because of the very slow IW growth rates found. It is our present purpose to present calculations of the implications of the theory using somewhat realistic Väisälä profiles (emphasizing the upper ocean waters) and the SW relaxation model of Watson (1986). Unless otherwise specified, the GM Väisälä frequency model is chosen here for all of our calculations:

$$N(z) = \begin{cases} 0, & 0 > z > -D, \\ N_0 \exp[(z + D)/B], & -D > z > -B_b \end{cases}$$

$$B = 1200\ \mathrm{m}, \quad N_0 = 0.01\ \mathrm{sec}^{-1}. \quad (4.21)$$

We shall, however, describe some calculations done with a "Patchex" model and also with a constant N model. The mode functions $W_{j,K}$ were evaluated numerically from (2.3) using both a WKB approximation (where valid) and numerical integration of the differential equation. The results from use of the relaxation model (3.13) were compared with those using the δ-function limit (4.12). Generally, the two sets of calculations were within a "factor of two" range of agreement, those done with the relaxation model tending to be somewhat larger. It should be noted in this context that when β is large Δ is small, and when β is small Δ can be replaced by the δ-function. The short waves for which β is large do not contribute strongly to the coupling. Thus, we do not expect dramatically different results from the two models. For consistency with the condition (2.1) we have limited the integration in (4.10) and (4.16) to the domain $k > K$. This constraint did not seem to affect our numerical results, however.

In Fig. 1 we show the e-folding rate $\nu(\theta_w)$ [defined in (4.18) and expressed in days^{-1}] for a mixed layer depth $D = 20$ m, a wind speed $W = 10$ m s^{-1}, and the first vertical mode corresponding to $j = 1$. The curves are labeled by the value of KB. The striking feature here is that the energy transfer is overwhelmingly from the IW field to the SW field. Although ν_s (4.16) is positive definite, the net rate is strongly dominated by the

[3] It might be noted that to evaluate the mean rates it is easiest to first do an analytic integration of (4.10) and (4.16) over θ_w before integrating over k. To verify our numerical evaluations, we have done this and also integrated over wind angles last, as implied by (4.14) and (4.17).

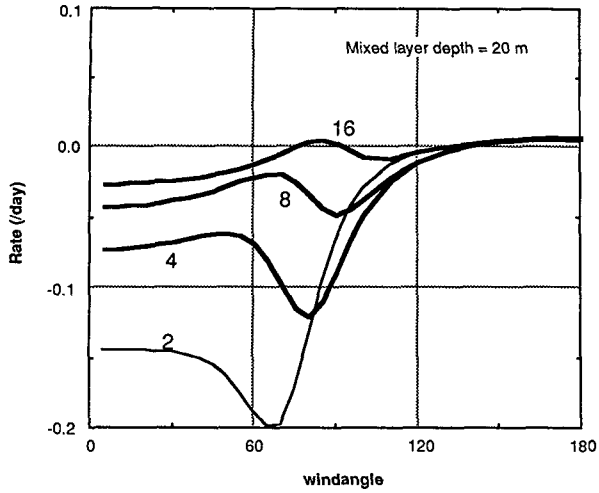

FIG. 1. The e-folding rate (day^{-1}) (4.18) is shown as a function of wind angle θ_w (with respect to the direction of horizontal propagation of the internal wave) for several values of KB and the mode $j = 1$. The surface wave spectrum is that given by (2.19), (2.20), and (2.21), and the wind speed is 10 m s^{-1}. Positive rates correspond to internal wave growth, negative rates to internal wave decay.

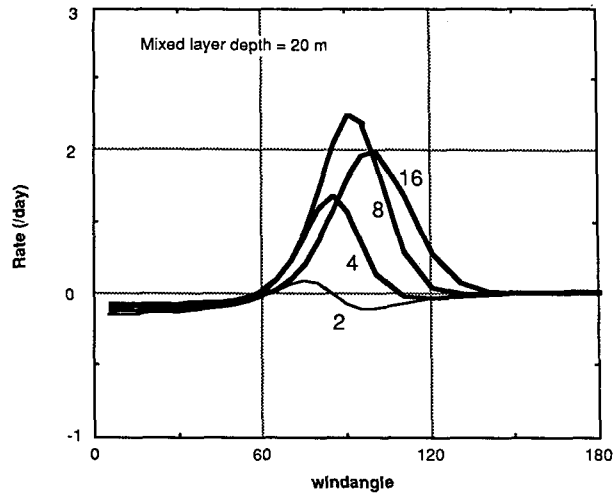

FIG. 3. As in Fig. 1, except that the wind speed is 20 m s^{-1}.

contribution from the modulation mechanism. The small positive value of ν at certain angles θ_w is sensitive to the SW spectral model, as was observed by DD. This is illustrated in Fig. 2, where the above calculation is repeated using the "collimated" SW model (2.22). The possibility of IW growth at certain angles is much more pronounced in this case.

In Fig. 3 we repeat the calculation of Fig. 1, but with a wind speed $W = 20$ m s^{-1}. Except for $KB = 2$, the pronounced effect is IW growth, or energy transfer from the SW field to the IW field. In Fig. 4 we repeat the calculation of Fig. 3 using the collimated SW model (2.22), but with $D = 60$ m. An even more pronounced growth of the IW field is seen.

There are two reasons for the significant difference between wind speeds of 10 and 20 m s^{-1}. First, at higher wind speeds $\nu_m(\theta_w)$ tends to have a greater range of positive values; second, ν_s grows rapidly with increasing wind strength.

In Fig. 5 we show the average growth rate (4.19) as a function of wind speed. Here, again, the mode corresponds to $j = 1$ and the curves are labeled by the IW horizontal wavelength expressed in meters. The same calculation is repeated in Fig. 6, but with a mixed layer depth $D = 60$ m. We see from these results that for $W < 15$ m s^{-1} or for longer wavelengths the predominant effect is to transfer energy from the IW field to the SW field. This contrasts with the view frequently expressed

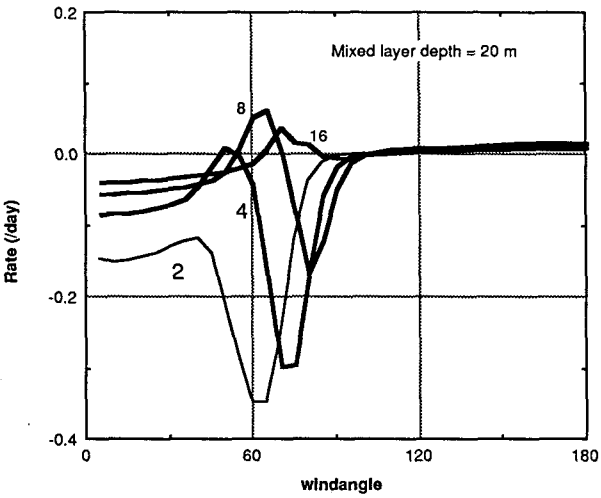

FIG. 2. The e-folding rate is shown for the same conditions as in Fig. (1), except that the collimated spreading function (2.22) is used.

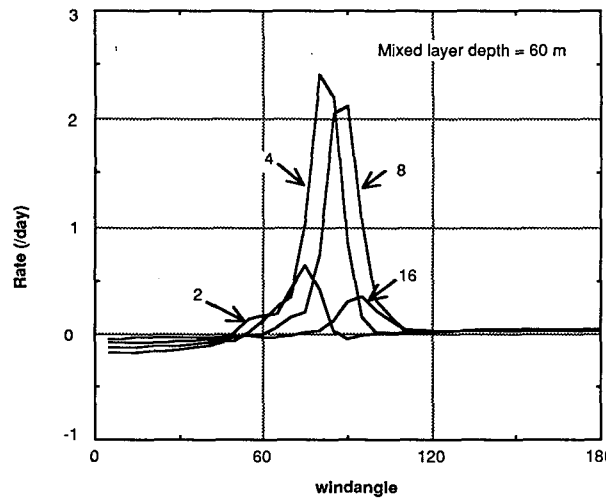

FIG. 4. As in Fig. 2, except that the wind speed is 20 m s^{-1} and the mixed layer depth has been changed as indicated.

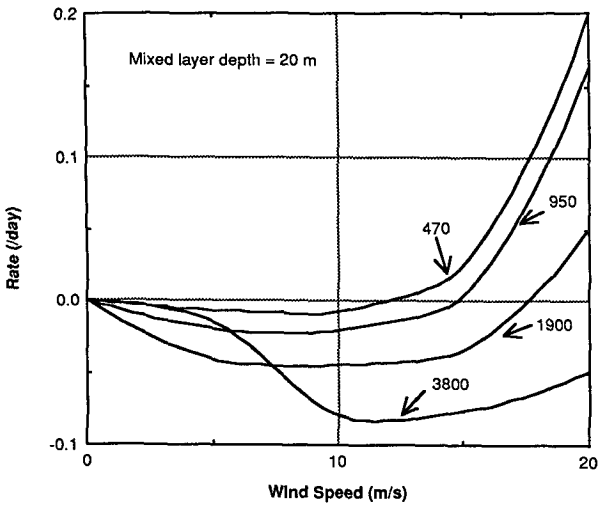

FIG. 5. The mean e-folding rate (day^{-1}) (4.19) is shown for several IW horizontal wavelengths (expressed in meters) and mode $j = 1$ as a function of wind speed. The SW spectrum is that of (2.21).

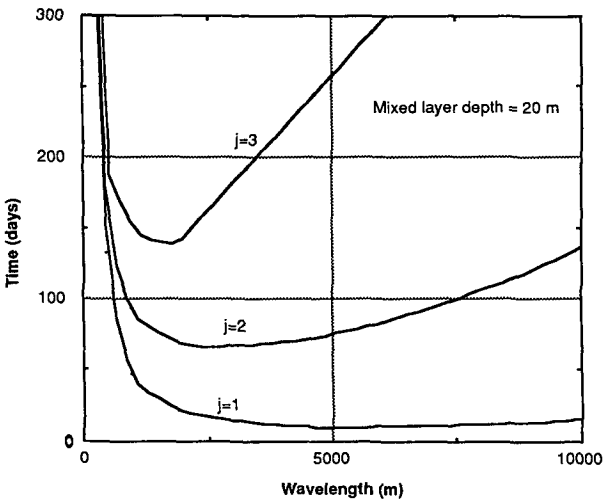

FIG. 7. The decay time [the negative of the inverse of the expression (4.19) expressed in days] for the internal wave field is shown as a function of IW horizontal wavelength and a wind speed of 10 m s^{-1}. Results are shown for the first three vertical modes and the surface wave spectrum is that of (2.21).

that wind waves tend to generate internal wave energy, however slowly.

In Figs. 7 and 8 we show the IW decay time ($= -\nu^{-1}$), expressed in days, as a function of the IW horizontal wavelength and for $j = 1, 2, 3$. The wind speed is 10 m s^{-1} and $D = 20$ and 60 m. Although not shown, the decay time for $j = 1$ increases with horizontal wave length for lengths greater than 15 km.

For the first mode, corresponding to $j = 1$, the time scales presented here tend to be significantly less than the 50 to 100 day decay times quoted in the Introduction. The decay times for the second mode tend to lie in this 50 to 100 day range. For the higher modes the energy exchange between the SW and IW fields does not appear to be very significant.

In Fig. 9 we show the ratio

$$\left|\frac{\nu_s}{\nu_m}\right|$$

as a function of wind speed for several IW horizontal wavelengths and $D = 60$ m. When $W < 15$ m s^{-1} the contribution of the spontaneous mechanism to the net energy exchange is seen to be negligible.

The power delivered to the SW field from the IW field,

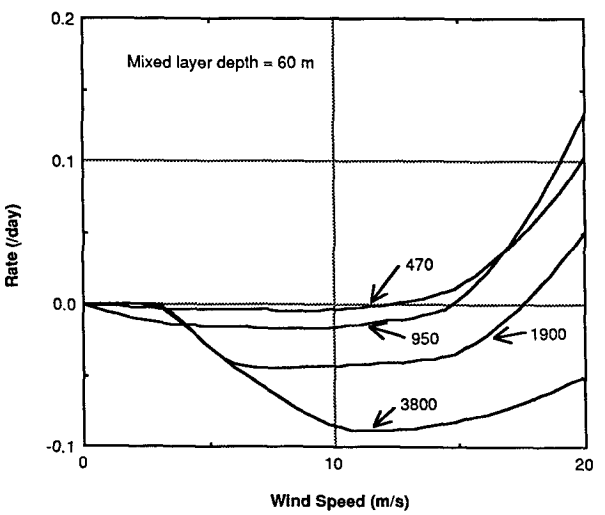

FIG. 6. As in Fig. 5, except for the indicated change in mixed layer thickness.

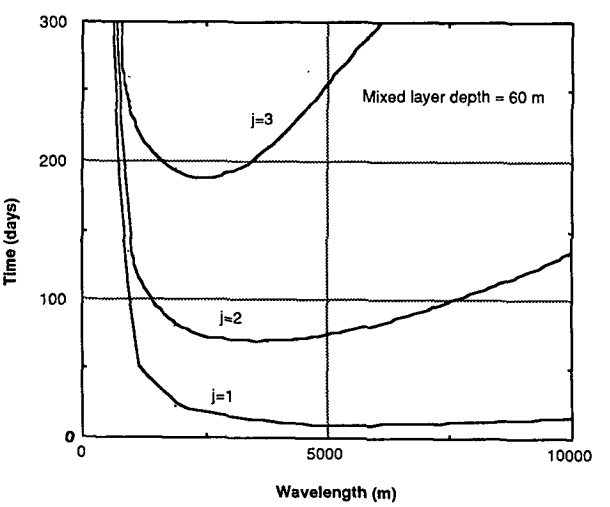

FIG. 8. As in Fig. 7, except that the mixed layer depth is changed as indicated.

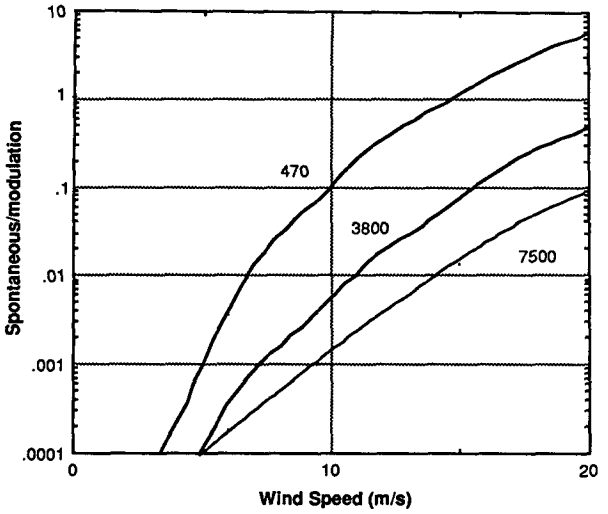

FIG. 9. For the data obtained for Fig. 6 we show the ratio of contributions from the spontaneous and modulation mechanisms as a function of wind speed for several IW horizontal wavelengths (expressed in meters).

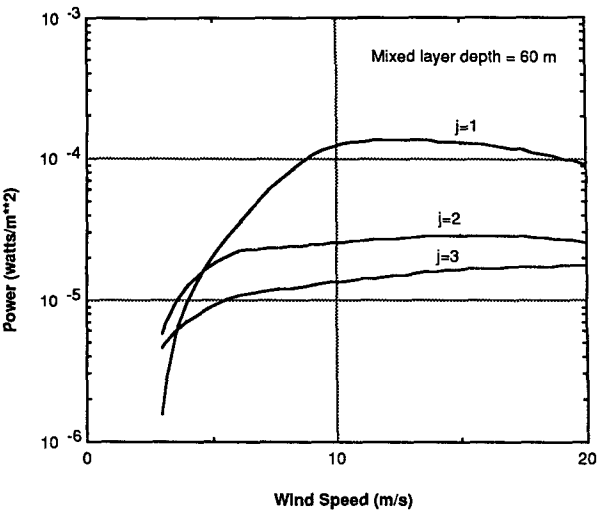

FIG. 10. The power per unit area (4.23) extracted from the IW field by the SW field shown as function of wind speed for the first three vertical modes. The SW spectrum is that specified by (2.21).

$$P(j) = -\int_{K_0}^{\infty} P(j, K)dK, \qquad (4.23)$$

is shown as a function of wind speed in Fig. 10. The curves are labeled by the mode number j. The mixed layer depth is 60 m and we have taken $K_0B = 0.5$. The total GM energy (2.12) for the first mode in this wavelength range is about 70 J m^{-2}, so a few days are required to deplete this mode when the wind speed is in the 10 m s^{-1} range.

The dependence of $\bar{\nu}$ on mixed layer depth D is shown in Fig. 11 for several selected IW horizontal wavelengths and $j = 1$. The wind speed here is 10 m s^{-1}. The variation of the rates ν with D is dominated by the exponential factor $\exp(KD)$ in (2.3).

We have examined several data sets for $N(z)$ taken by Pinkel[4] during the Patchex experiment. Representative of some of these is a strong thin thermocline at 50 m depth superimposed on a Väisälä profile similar to (4.21). We model this thermocline as a density discontinuity of strength

$$\int_{\text{thermocline}} N^2 dz = 0.035 \text{ m s}^{-2}.$$

The IW decay time for this "Patchex" profile is shown in Fig. 12 for a wind speed of 10 m s^{-1}. These results are seen to differ little from those of Fig. 8. The energy transfer rates are certainly sensitive to gross variations in the Väisälä profile, however.

To see the effects of a significant change in the Väisälä profile we consider the model

$$N(Z) = \begin{cases} 0, & 0 > Z > -50 \text{ m} \\ N_0 = 0.01, & -50 \text{ m} > Z > -1000 \text{ m}, \end{cases}$$

with the ocean bottom at 1000 m depth. The resulting IW decay times are shown in Fig. 13.

To illustrate the significance of our calculations, we refer to Table 1, where yearly means for wind speed and mixed layer thickness are quoted for three locations on the North Pacific Ocean. We recognize that the mixed layer is much more complex than accounted for in our model and can vary significantly in a day's time, as can the wind. Reference to Figs. 8 and 10 does,

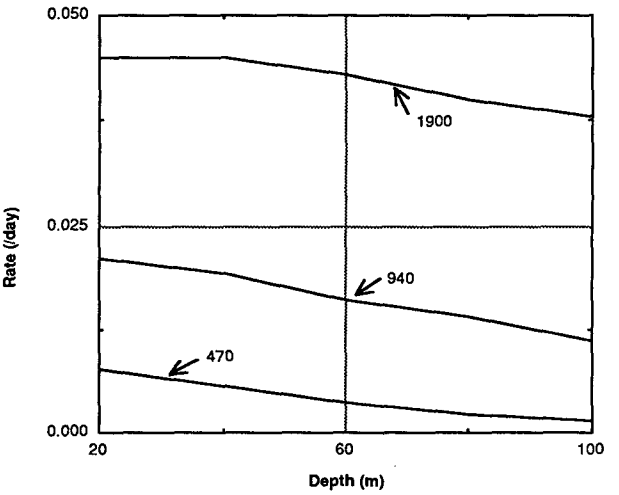

FIG. 11. The negative of the e-folding rate (4.19) shown as a function of mixed layer depth for $j = 1$, a wind speed of 10 m s^{-1}, and the SW spectrum (2.21). The curves are labeled by the IW horizontal wavelength.

[4] We are indebted to Dr. Pinkel for the use of this data.

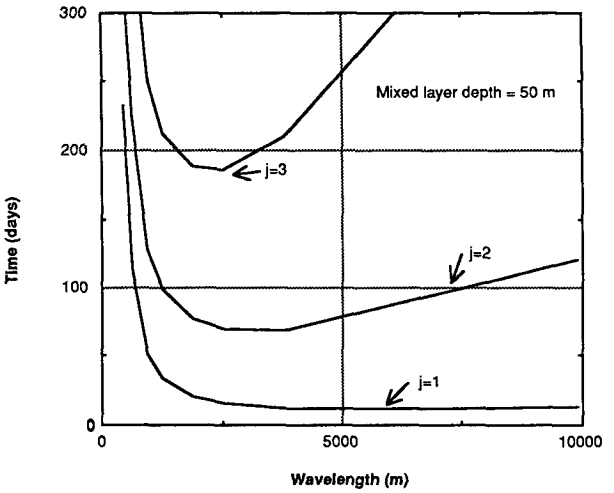

FIG. 12. The IW decay time is shown for the same conditions as those of Fig. 7, except that the "Patchex" Väisälä profile is assumed.

however, suggest that for these areas the first mode internal wave should decay rapidly, if no source for maintaining this exists. To be more precise, we are led to expect IW decay within, perhaps, 10 to 20 days for internal waves in the wavenumber–frequency range:

horizontal wavelength:	1 to 20 km	
vertical wavelength:	>1 km	
frequency/N_0:	0.15 to 0.7.	(4.24)

Theories for the transport of internal wave energy imply that the long vertical wavelength (low mode number) waves act as a source of energy which flows to higher mode numbers, where shear instabilities lead to turbulent dissipation (for example, see Gregg 1989). McComas (1978) conjectured on the basis of the work

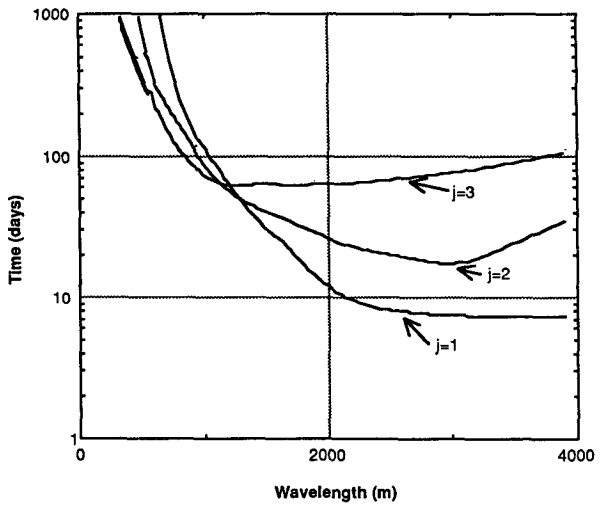

FIG. 13. As in Fig. 12, except a constant Väisälä profile is assumed.

TABLE 1. Yearly average wind speed and mixed layer thickness* for three areas of the North Pacific Ocean. Data taken from the 1989 U.S. Pilot Charts.

Location	Mean wind speed (m s^{-1})	Average mixed layer thickness (m)
50°N, 175°W	9.0	50
35°N, 165°W	7.5	45
25°N, 135°W	6.7	70

* Robinson, M., 1976: Atlas of the North Pacific Ocean Monthly Mean Temperatures and Mean Salinities of the Surface Layer. Naval Oceanographic Office.

Reid, J. (private communication) data from 1966 Boreas Expedition.

Reid, J., 1982: On the use of dissolved oxygen concentrations as an indicator of vinter convection. Naval Research Reviews, No. 3.

of McComas and Bretherton (1977) that the high frequency-low mode number region of the IW spectrum is fed by an external energy source and that this energy flows to lower frequency and high mode numbers. The detailed studies of energy balance within the IW spectrum made by McComas and Bretherton (1977) and by Pomphrey et al. (1980) were not, however, extended into the high frequency domain where we find strong SW–IW interactions. The careful analysis of Flattè et al. (1985) also did not address this high frequency domain. The injection of energy from mesoscale current shears into the IW field occurs within the inertial frequency band, according the calculations of Watson (1985). Bell (1978) has given a calculation that suggests that energy can be injected into the internal wave field at high frequency and low mode numbers by mixed layer flow. Rates could not be given with confidence by Bell because of a lack of knowledge of the relevant environmental parameters.

We are left with an unclear picture of the energy source (of sources) required to maintain the internal wave spectrum in the domain (4.24), and in fact of the actual levels of internal wave energy in this domain.

5. Generation by ocean swell

Several observations have been reported (for example, see Apel et al. 1975; Briscoe 1983) which suggest that a strong ocean swell may generate internal waves. Generation by a sharply collimated swell was investigated by DD, who found IW growth for a sufficiently narrow SW spreading function and a sharp thermocline Väisälä model.

In this section we illustrate IW generation from a narrow band SW system by two mechanisms. The first is the modulation mechanism as described by (4.10). The second is generation from a swell wave field that has a prescribed modulation (not resulting from IW interactions). Equation (3.15) is used to calculate IW generation by this mechanism. We can use the exact resonance condition (4.12) for both of these because of the relatively long wavelength of ocean swell.

For the first mechanism described above, we replace (2.19) by

$$S(k) = \left[\frac{\langle \zeta^2 \rangle}{\sqrt{2\pi}\,\Delta k}\right] \exp[-(k - k_p)^2/(2\Delta^2)], \quad (5.1)$$

where Δ and k_p are parameters. It is supposed that

$$\Delta \ll k_p.$$

Equation (2.20) is used for the spreading function and it is now assumed that

$$\sigma \gg 1.$$

We replace the angle θ_w in G by θ_s to indicate that this is the angle between the direction of swell propagation and that of K.

Conditions (5.2) and (5.3) permit an analytic evaluation of (4.10). If we choose θ_s to give maximum IW growth rate (that is, approximately 90°) we obtain

$$\text{Rate (day}^{-1}) = 1.7 \times 10^5 \,\text{Re}(p) = \frac{1.9 \times 10^4 \langle \zeta^2 \rangle k_p^2 \alpha \sigma^2}{(KB)^2 H}\left(\frac{\Omega^2}{Kg}\right), \quad (5.4)$$

where

$$H = 1 + \left(\frac{2\sigma\Delta\Omega}{K\sqrt{gk_p}}\right)^{1.5}.$$

Here α is defined by (3.17).

To illustrate (5.4) we choose a swell wavelength of 145 m, $H = 1$, $\sigma = 10$, $\langle \zeta^2 \rangle k_p^2 = 0.04$, and the Väisälä profile (4.21). The growth times [that is, the reciprocal of (5.4)] for the first three modes are shown in Fig. 14. Reference to Fig. 4, which describes a similarly collimated spectrum, illustrates the sensitivity of the growth rate on the angle θ_s. It is seen that e-folding rates in the range of (1 day)$^{-1}$ may be expected.

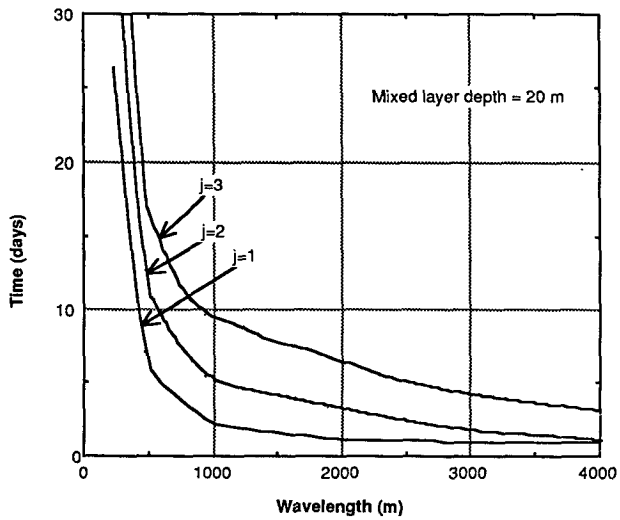

FIG. 14. The IW growth time [the reciprocal of (5.4), expressed in days] due to interaction with ocean swell is shown as a function of horizontal wavelength for the first three vertical modes.

To even a casual observer a swell wave train exhibits modulation in the direction of its propagation (as a time record taken at a fixed position would show). Because the resonance condition (3.3) requires that the swell angle θ_s be nearly 90°, we require modulation also along the wave crests. One might, for example, expect such modulation to be related to the width σ^{-1} of the spreading function. Snodgrass et al. (1966) have discussed a number of phenomena which may determine the swell spectrum, such as the dimensions of the region in which swell is produced, refraction by currents, and scattering from wind waves, islands, or shallow areas in the swell path.

We have not, however, found data from which to model F_s in (3.15), so are led to a very simplified model that illustrates the mechanism and permits analytic integration of (3.15). We consider the swell to be represented as a sequence of wave trains, each of length T and of the form:

$$F_s = \rho_0 V_k \Psi(x, k, t),$$

$$\Psi = M(x, t) S(k) G(\theta - \theta_s),$$

$$M(x, t) = \sum_L P(L)\{1 + e^{-t/T}\cos[L \cdot (x - c_g)]\}, \quad (5.5)$$

where $t > 0$ and

$$\sum_L P(L) = 1.$$

Here c_g is the group velocity of the swell and we suppose that P describes modulation along the swell crests.

To continue, we assume that E_i in (3.15) represents the IW energy in a restricted band which matches the resonance condition (3.3). The current U is that due to this restricted IW band. For S in (5.5) we use (5.1).

Equation (3.15) may be integrated analytically for a narrow band collimated swell. We define the average power received by the IW field as

$$\text{power} = E_i/T, \quad (5.6)$$

which is appropriate if swell groups such as (5.5) arrive at intervals T. We find from (3.15) that

$$\text{power} = 0.25\rho_0 (N_0 B)^2 B\alpha(\Omega/N_0)(T\omega_{k_p})^2 \times [\langle \zeta^2 \rangle / B^2]^2 (\bar{P}^2/(KBT)). \quad (5.7)$$

Here $\bar{P}$ is the weighted sum of $P(K)$ over the specified IW band.

To illustrate (5.6) we take $k_p = 2\pi/145$ m^{-1}, $T = 100$ s and $\langle \zeta^2 \rangle = 20$ m^2. The quantity

$$\text{power}/\bar{P}^2$$

is shown in Fig. 15 for the first three modes. We see from these results that if the swell modulation well

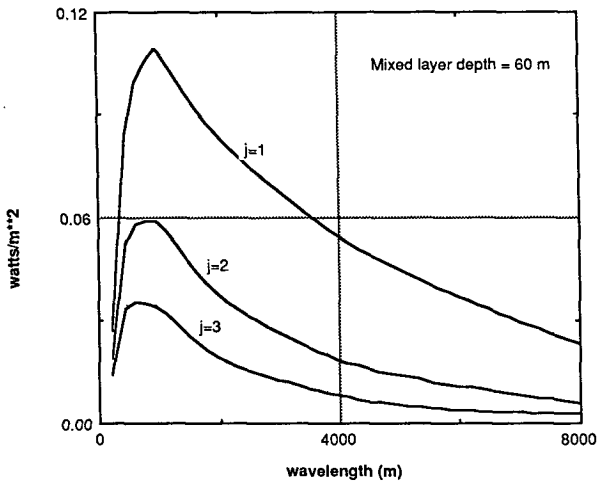

FIG. 15. The IW power per unit area received from a modulated ocean swell (5.7) is shown for the first three vertical modes as a function of horizontal wavelength.

matches the IW field that rather intense generation of internal waves can result.

6. Nonlinear modulation of surface waves

In this section we shall investigate the interaction of surface waves with an IW packet that has a finite extent in the x-direction, but is uniform in the y-direction. A finite packet of internal waves may arise from statistical fluctuations in the ambient field, from uneven topography, or a transient source. In the interest of numerical simplicity we shall set $S = 0$ in (3.9). Damping will be accounted for by ignoring those portions of the SW spectrum for which a significant SW–IW interaction time T_i is greater than the relaxation time, or

$$T_i > \beta^{-1}(k). \tag{6.1}$$

We express the IW surface current U in the form

$$\mathbf{U} = \mathbf{i}U_0 V(\xi). \tag{6.2}$$

It is supposed that

$$V \approx 0 \quad \text{for} \quad \xi < \xi_1 \quad \text{or} \quad \xi > \xi_2 \tag{6.3}$$

and that within the range $\xi_1 < \xi < \xi_2$

$$V \approx \cos(K\xi). \tag{6.4}$$

We may now write (3.9) in the form

$$\left[\dot{\xi}\frac{\partial}{\partial \xi} + \dot{k}_x \frac{\partial}{\partial k_x}\right] F_s = 0, \tag{6.5}$$

where

$$\dot{\xi} = C_g(\mathbf{k})(k_x/k) - C_I + U_0 V(\xi),$$

$$\dot{y} = C_g(\mathbf{k})(k_y/k),$$

$$\dot{k}_x = -k_x U_0 \frac{\partial V}{\partial \xi},$$

$$\dot{k}_y = 0. \tag{6.6}$$

We shall consider only surface waves which travel in the positive x-direction and overtake the packet. For those waves which have not yet reached the IW packet, say at time t_0 and position $\xi < \xi_1$, we have

$$F_s = F_a. \tag{6.7}$$

Similarly, we have

$$\mathbf{k} = \mathbf{k}_0, \quad \text{a constant for} \quad t < t_0. \tag{6.8}$$

Then having integrated the ray equations (6.6) to a point (k, ξ) within the packet we may set

$$F_s(\mathbf{k}, \xi) = F_a(\mathbf{k}_0). \tag{6.9}$$

A simple technique for evaluating $F_s(k, \xi)$ is to choose a specific value of (k, ξ) and to integrate (6.6) backward in time to a location $\xi < \xi_1$. For $\xi < \xi_1$, we know that $k = k_0$. Then with the use of (6.9) we obtain immediately the numerical value of $F_s(k, \xi)$.

On integrating (6.6) we must distinguish four trajectory types:

1) those which pass through the packet from ξ_1 to ξ_2

2) those which have entered the packet at ξ_1, and are turned back at the point where $d\xi/dt = 0$ [equivalent to the resonance condition (3.4)], and then pass back out of the packet at $\xi = \xi_1$.

3) those which have been overtaken by the packet at $\xi = \xi_2$

4) those which are trapped within the packet.

We shall ignore the type 3 and type 4 trajectories. We must, however, calculate the type 1 and type 2 trajectories. The type 1 trajectories do not lead to an energy exchange between the two fields, since on emerging from the packet a SW has the same wavenumber as it had on entering.

The rate of energy exchange to the IW field is obtained from (3.8) and (6.9) as

$$\dot{E}_i(j, K) = -U_0 K \int_{\xi_1}^{\xi_2} d\xi \Big/ L_x \int d^2k c_x k_x \times \sin(K\xi) F_s(\mathbf{k}, \xi). \tag{6.10}$$

Here we have taken $L_x = \xi_2 - \xi_1$.

As a first example we set

$$V(\xi) = 1.46 \cos(K\xi)/\{[1 + \exp(-0.5K\xi)] \times [1 + \exp(0.5K\xi - 6.28)]\} \tag{6.11}$$

and take (here λ_I is the internal wave wavelength)

standard profile (4.21)

$D = 20$ m

$$U_0 = 0.25 \text{ m s}^{-1}$$
$$c_I = 0.56 \text{ m s}^{-1}$$
$$\lambda_I = 470 \text{ m}$$
$$\theta_w = 30°. \quad (6.12)$$

This is a strong internal wave, corresponding to a vertical displacement at the thermocline of 8 m.

The resulting modulation function $M(k, \xi)$ [see (2.17)] is shown as the solid curves in Fig. 16 for the location $K\xi = 3\pi$. The lines are labeled by the direction of k and shown as functions of k. The corresponding results obtained from linear perturbation theory (4.4) are represented by the dashed lines. The blocking of the SW field is seen at those values of k where M vanishes.

To study the energy transfer (6.10) we take

$$V(\xi) = \begin{cases} \cos(K\xi), & \pi/2 < K\xi < 5\pi/2 \\ 0, & \text{outside above range,} \end{cases} \quad (6.13)$$

and continue to use the parameters given in (6.12).

We have seen that waves having type (1) trajectories may be excluded from the integrand in (6.10). We also exclude those type (2) waves for which the time

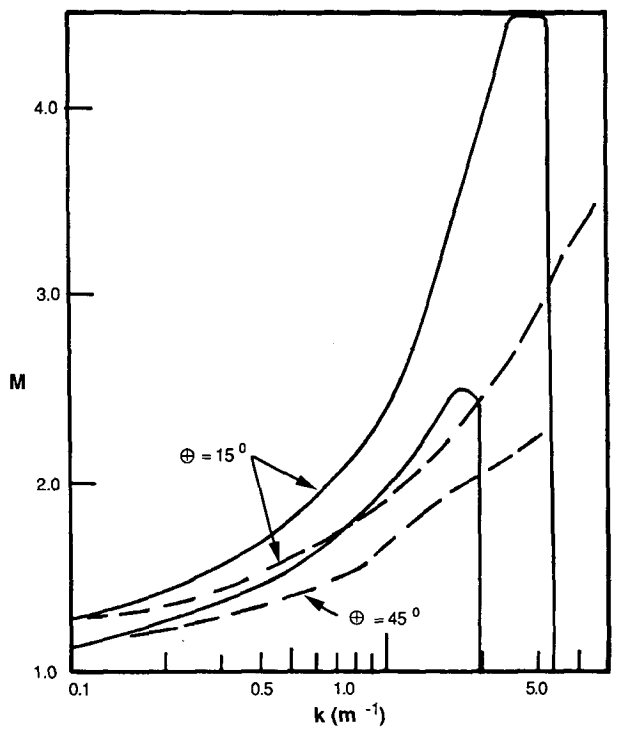

FIG. 16. The modulation function $M(K, \xi)$ is shown for the parameters (6.12) and a location corresponding to $K\xi = 3\pi$. The curves are labeled by the direction of k. The solid curves obtained using nonlinear theory, the dashed curves from the linearized equation (4.3).

T_i to propagate from $\xi = \pi/(2K)$ to the turning point exceeds β^{-1} [condition (6.1)]. We see, then, that just as in the linear theory of the last Section, the triad resonance condition must be met in order that energy be exchanged between the two fields.

Surface waves reaching the packet (6.13) encounter an IW current in the negative x-direction. This current tends to drive the surface waves back out of the packet. If there is a turning point, corresponding to $d\xi/dt = 0$, this will occur in the interval $\pi/2 < K\xi < \pi$. The adverse current does work on the SW field, so tends to increase the SW energy. This is seen mathematically in (6.10), since $M > 1$ and $\sin(K\xi)$ is positive in the interval $\pi/2 < K\xi < \pi$.

For the parameters given in (6.12) the expression (6.10) was evaluated. A characteristic time was obtained:

$$T_d = [\dot{E}_i(j, K)/E_i(j, K)]^{-1} = -24 \text{ days}. \quad (6.14)$$

For a mixed layer depth $D = 80$ m, we would have obtained $T_d = -70$ days. We note (see Fig. 16) that for this case waves near the spectral peak do not contribute to the energy exchange.

Because (6.9) is nonlinear, the coupling leads to spectral transfer within the IW field. For example, let us consider a second IW mode (j', K') for which

$$U' = U'_0 \cos(K'x - c'_I t + \alpha'). \quad (6.15)$$

The total IW current is the sum of (6.13) and (6.15). If, however, U'_0 is too small to significantly modulate F_s, then

$$E_i(j', K') = -U'_0 K' \int_{\xi_1}^{\xi_2} d\xi \Big/ L_x \int d^2k k_x c_x \sin(K'\xi) F_s(k, \xi) \quad (6.16)$$

where F_s is determined by (6.13) only. Evidently, depending upon the mode (j', K') either sign may be encountered in (6.16). The implication of this is that in the nonlinear regime, energy may be transferred among the IW modes through SW coupling.

7. Conclusions

We have described mechanisms for energy exchange between internal wave and surface wave fields. The important effect in the case of wind waves is the draining of energy from the IW field in the high frequency, long vertical wavelength domain. This would seem to be significant in assessing the factors which determine the total energy budget of the internal waves. In reviewing existing models which describe energy fluxes into and within the IW spectrum, we have tentatively identified mixed layer flows as a possible source of the required energy. Partial depletion of the IW spectrum

in the region of high energy loss and at times of high energy loss might occur.

We have not explored here the dependence of the energy exchange rates on the Väisälä profile. To realistically assess the implications for internal wave energy balance, measured upper ocean profiles of N for selected locations and seasons should be used. Also, this should be related to historical records of wind speed for these locations.

As concluded by DD, a well collimated ocean swell may play a different role in that this can lead to rapid IW growth. Although this may be locally significant, it is not expected to be important for the IW total energy budget.

We have mentioned that external sources of SW modulation, such as the envelope of swell, wind variability, and Langmuir cells, may lead to IW generation. Nonlinear modulation, such as SW blocking, has been seen to introduce new aspects relating to SW–IW coupling.

Acknowledgments. I would like to thank Dr. Robert Pinkel for discussions of upper ocean internal wave activity and Dr. Joseph Reid for discussions of upper ocean stratification. This work was supported in part by ONR Contract N00014-87-K-0010.

APPENDIX

Derivation of Equation (3.5)

To derive (3.5) we first note that in the mixed layer the flow can be represented by a velocity potential Φ of the form

$$\Phi = \phi_g(\mathbf{x}, z, t) + \phi_i(\mathbf{x}, z, t). \quad \text{(A1)}$$

Here $x = (x, y)$ is a vector in a plane of constant z. The term ϕ_g contains the high frequency, high wavenumber part of Φ associated with gravity waves, while ϕ_i contains the low frequency, low wavenumber part of Φ associated with internal waves. The vertical displacement of the ocean surface ζ, due to wave motion, can likewise be represented as a sum of a high frequency part ζ_g and a low frequency part ζ_i:

$$\zeta(x, t) = \zeta_g(x, t) + \zeta_i(x, t). \quad \text{(A2)}$$

The SW–IW coupling was obtained in WWC from Bernoulli's equation at the surface (here ∇_s is the horizontal component of ∇):

$$\frac{\partial \zeta}{\partial t} + \nabla_s \cdot (\zeta \nabla_s \Phi) = w \quad \text{at} \quad z = \zeta, \quad \text{(A3)}$$

where w is the vertical component of fluid velocity. On averaging (A3) over many realization of the SW field and on extracting the low frequency and low wavenumber part, WWC and DD obtained the relation [Eq. (2.12) of WWC or (6.3) of DD]

$$w_i = \frac{\partial \phi_i}{\partial z} = \langle \nabla_s \cdot (\zeta_s \nabla_s \phi_s) \rangle_{LF} \equiv \Gamma(\mathbf{x}, t), \quad \text{at} \quad z = 0. \quad \text{(A4)}$$

The symbol $\langle \ \rangle_{LF}$ here implies both the ensemble average over SW field realization and the low pass filter in frequency and wavenumber. Also, in (A4) only the second order triad terms are kept.

We may use (2.14) to re-express (A4) in terms of the SW action density (as was done by DD):

$$\Gamma(\mathbf{x}, t) = \nabla_s \cdot \int d^2k \mathbf{k} F_s(\mathbf{x}, \mathbf{k}, t)/\rho_0. \quad \text{(A5)}$$

This will be recognized as the gradient of the SW momentum per unit area. It represents the driver of internal wave excitation.

To satisfy the condition (3.6) WWC generalized (2.4):

$$w_i(\mathbf{x}, 0, t) = \sum_{j,\mathbf{K}} e^{i\mathbf{K}\cdot\mathbf{x}} A_{j,\mathbf{K}} W_{j,K}(0) + \Gamma(\mathbf{x}, t). \quad \text{(A6)}$$

They then obtained a set of differential equations for the amplitudes Aj, k. On rewriting these in terms of the U of (2.7) we obtain (3.5).

REFERENCES

Apel, J. K., H. M. Byrne, J. R. Proni and R. L. Charnell, 1975: Observations of oceanic internal and surface waves from the Earth Resources Technology Satellite. *J. Geophys. Res.*, **80,** 865–881.

Ball, F. K., 1964: Energy transfer between external and internal gravity waves. *J. Fluid Mech.*, **19,** 465–478.

Bell, T. H., 1975: Topographically generated internal waves in the open ocean. *J. Geophys. Res.*, **80,** 320–327.

——, 1978: Radiation damping of inertial oscillations in the upper ocean. *J. Fluid Mech.*, **88,** 289–308.

Brekhovskikh, L. M., V. Goncharov, V. Kurtepov and K. Naugolnykh, 1972: Resonant excitation of internal waves by nonlinear interactions of surface waves. *Atmos. Oceanic Phys.*, **8,** 112–117.

Briscoe, M. G., 1983: Observations on the energy balance of internal waves during Jasin. *Phil. Trans. Roy. Soc. London,* **A308,** 427–444.

Curtin, T. B., and C. N. K. Mooers, 1975: Observation and interpretation of a high frequency internal wave packet and surface slick pattern. *J. Geophys. Res.*, **80,** 882–894.

Donelan, M. A., J. Hamilton and W. H. Hui, 1985: Directional spectra of wind-generated waves. *Phil. Trans. Roy. Soc. London,* **A315,** 509–562.

Dysthe, K. B., and K. P. Das, 1981: Coupling between a surface wave spectrum and an internal wave: modulational interaction. *J. Fluid Mech.*, **104,** 483–503.

Flattè, S. M., F. S. Henyey and J. A. Wright, 1985: Eikonal calculations of short-wavelength internal-wave spectra. *J. Geophys. Res.*, **90,** 7265–7272.

Fu, L. L., and B. Holt, 1984: Internal waves in the Gulf of California: Observations from a spaceborne radar. *J. Geophys. Res.*, **89,** 2053–2060.

Garget, A. E., P. J. Hendricks, T. B. Sanford, T. R. Osborn and A. J. Williams, 1981: A composite spectrum of vertical shear in the upper ocean. *J. Phys. Oceanogr.*, **11,** 1258–1271.

Garrett, C., and W. Munk, 1972a: Space-time scales of internal waves. *Geophys. Fluid Dyn.*, **2**, 225–264.

——, and ——, 1972b: Ocean mixing by breaking internal waves. *Deep-Sea Res.*, **19**, 823–832.

Gill, A. E., 1984: On the behavior of internal waves in the wake of storms. *J. Phys. Oceanogr.*, **14**, 1129–1151.

Gregg, M., 1987: Diapycnal mixing in the thermocline: A review. *J. Geophys. Res.*, **92**, 5249–5286.

——, 1989: Scaling dissipation in the thermocline. *J. Geophys. Res.*, **94**, 9686–9698.

——, E. D'Asarro, T. Shay and N. Larson, 1986: Observations of persistent mixing and near-inertial waves. *J. Phys. Oceanogr.*, **16**, 856–885.

Hasselmann, K., 1967: Nonlinear interactions treated by the methods of theoretical physics. *Proc. Roy. Soc.*, **A299**, 77–99.

——, 1968: Weak-interaction theory of ocean waves. *Basic Developments in Fluid Mechanics*, Vol. 2, 117–182. M. Holt, Ed., Academic Press.

Hughes, B. A., 1978b: The effects of internal waves on surface wind waves. 2. Theoretical analysis. *J. Geophys. Res.*, **83**, 455–465.

——, and H. L. Grant, 1978a: The effects of internal waves on surface wind waves. 1. Experimental measurements. *J. Geophys. Res.*, **83**, 443–454.

Kanthu, L. H., 1979: On generation of internal waves by turbulence in the mixed layer. *Dyn. Atmos. Oceans.*, **3**, 39–46.

Kenyon, K. E., 1968: Wave-wave interactions of surface and internal waves. *J. Mar. Res.*, **26**, 208–231.

Leaman, K. D., 1976: Observations on the vertical polarization and energy flux of near-inertial waves. *J. Phys. Oceanogr.*, **6**, 894–908.

——, and T. B. Sanford, 1975: Vertical energy propagation of internal waves: a vector spectral analysis of velocity profiles. *J. Geophys. Res.*, **80**, 1975–1978.

Lueck, R. G., W. R. Crawford and T. R. Osborn, 1983: Turbulent dissipation over the continental slope off Vancouver Island. *J. Phys. Oceanogr.*, **13**, 1809–1818.

McComas, C. H., 1978: Equilibrium mechanisms within the oceanic internal wave field. *J. Phys. Oceanogr.*, **7**, 836–845.

——, and F. P. Bretherton, 1977: Resonant interactions of oceanic internal waves. *J. Geophys. Res.*, **82**, 1397–1412.

——, and P. Muller, 1981: The dynamic balance of internal waves. *J. Phys. Oceanogr.*, **11**, 970–986.

Munk, W. H., 1981: Internal waves and small scale processes. *Evolution of Physical Oceanography*, B. Warren and C. Wunsch, Eds., The MIT Press, 264–270.

Olbers, D. J., and K. Herterich, 1979: The spectral energy transfer from surface waves to internal waves. *J. Fluid Mech.*, **92**, 349–380.

Osborn, T., 1978: Measurements of energy dissipation adjacent to an island. *J. Geophys. Res.*, **83**, 2939–2957.

Phillips, O. M., 1973: On the interactions between internal waves and surface waves. *Atmos. Oceanic Phys.*, **9**, 565–568.

——, 1977: *The Dynamics of the Upper Ocean.* Cambridge University Press.

——, 1984: On the response of short ocean wave components at a fixed wavenumber to ocean current variations. *J. Phys. Oceanogr.*, **14**, 1425–1433.

——, 1985: Spectral and statistical properties of the equilibrium range in wind-generated gravity waves. *J. Fluid Mech.*, **156**, 505–531.

Pinkel, R., 1985: A wavenumber-frequency spectrum of upper ocean shear. *J. Phys. Oceanogr.*, **15**, 1453–1469.

Pomphrey, N., J. D. Meiss and K. M. Watson, 1980: Description of nonlinear wave interaction using Langevin methods. *J. Geophys. Res.*, **85**, 1085–1094.

Snodgrass, F., G. Groves, K. Hasselmann, G. Miller, W. Munk and W. Powers, 1966: Propagation of ocean swell across the Pacific. *Phil. Trans. Roy. Soc. London*, **259A**, 431–497.

Thorpe, S. A., 1966: On wave interactions in a stratified fluid. *J. Fluid Mech.*, **24**, 737–751.

van Gastel, K., 1987: Imaging by x-band radar of subsurface features: a nonlinear problem. *J. Geophys. Res.*, **92**, 11857–11865.

Watson, K. M., 1985: Interaction between internal waves and mesoscale flows. *J. Phys. Oceanogr.*, **15**, 1296–1311.

——, 1986: Persistence of a pattern of surface gravity waves. *J. Geophys. Res.*, **91**, 2607–2615.

——, B. J. West and B. I. Cohen, 1976: Coupling of surface and internal gravity waves: a mode coupling model. *J. Fluid Mech.*, **77**, 185–208.

Wigner, E. P., 1932: On the quantum correction for thermodynamic equilibrium. *Phys. Rev.*, **40**, 749–759.